Chen Zheng, Wenlin Feng\*, Xiaozhan Yang, Bangxing Li and Zhi Chen\*

# Silver-coated three-core fiber Michelson interferometer for liquid-level measurement

https://doi.org/10.1515/zna-2020-0201 Received July 25, 2020; accepted October 2, 2020; published online October 27, 2020

**Abstract:** The Michelson liquid-level sensor based on silver coated the end face of the three-core fiber reflection structure has been proposed to measure continuous or discrete liquid level. The Michelson interference structure can be obtained by the combination of the single-mode optical fiber and the three-core optical fiber with the silver film coated on the other end face of it. The inter-mode interference can be obtained by the fiber-core mismatch at the fusion joint. The liquid level can be measured by monitoring the dip wavelength shift of the interference spectrum. The results indicate that the sensitivity of the liquid-level sensor will decrease with the increasing sensing length. The sensing length of 30 mm is selected to investigate the performance of the sensor. The sensitivity of water level is reached as high as 392.83 pm/mm with an excellent linearity of 0.99946. Interestingly, the sensitivity of the sensor increases with the liquid refractive index and the sensitivity of the refractive index for NaCl solution is 4410.74 pm/mm/RIU. The performance of the sensor is very stable in the range of 20-90 °C. The maximum drift for temperature is 0.3001 nm. The sensor can be applied to the measurement of the liquid level in different environments.

Keywords: optic-fiber sensor; liquid-level sensing; Michelson interference: three-core fiber.

E-mail: z.chen@cgut.edu.cn

Chen Zheng, College of Science, Chongqing University of Technology, Chongqing 400054, China

Xiaozhan Yang and Bangxing Li, College of Science, Chongqing University of Technology, Chongqing 400054, China; Chongqing Key Laboratory of Green Energy Materials Technology and Systems, Chongging 400054, China

#### 1 Introduction

Liquid-level sensor has been widely used in many fields, such as petrochemical, biopharmaceutical and tidal lake water-level monitoring. The sensor often work in the complex and changeable ambient conditions, for example, the strong electromagnetic interference, inflammable, explosive, corrosive and low temperature, etc. [1-5]. The traditional sensors based on capacitance have to work under the electric power, which easily leads to security risks by the leakage of electric power [2-5]. Moreover, the traditional sensors based on electrical sensing technology cannot work accurately under the conditions of dynamics, large temperature variation and harsh environment [6]. Compared with other electrochemical liquid-level sensors, optic-fiber liquid-level sensors have the advantages of safety, low cost and variety application environments [7– 10]. Therefore, the research on optical fiber liquid-level sensors has great practical application value in daily life, military aerospace and other fields [11–14].

The general mechanism of optic-fiber Michelson sensor is the interference between two optical signals with the same wavelength and a relative phase difference. This phase difference is caused by the transmission of light in different media or along different path lengths [15]. This structure has the advantages of compact and simple manufacturing process. In recent years, there were many reports of optical fiber liquid-level sensors based on the utilization of Michelson interference structure. Rong et al. proposed a fiber-optic quasi-Michelson liquid-level sensor composed of a small-core fiber and single-mode fiber (SMF) coated with a silver reflective film. This sensor had a simple structure with low sensitivity of -68.3 pm/mm [16]. Li, et al. proposed a Michelson liquid-level sensor based on an optical fiber with core-offset structure [17]. Although the sensitivity of liquid-level sensor was increased to 77 pm/mm, the complexity of fusion process of the core offset structure hindered the repeatability of the experiment. They also did not study the temperature stability of the sensor. Liang, et al. used a self-made dual-mode elliptical multilayer core fiber (EMCF) and a SMF coated with a silver film to obtain a fiber-optic Michelson sensor [18], but the sensitivity to liquid level is not very high, and the highest sensitivity is only 48.93 pm/mm.

<sup>\*</sup>Corresponding authors: Wenlin Feng, College of Science, Chongqing University of Technology, Chongqing 400054, China; and Chongqing Key Laboratory of Green Energy Materials Technology and Systems, Chongqing 400054, China, E-mail: wenlinfeng@126.com; and Zhi Chen, School of Chemistry and Chemical Engineering, Chongqing University of Technology, Chongqing 400054, China,

Here, a simple Michelson liquid-level sensor based on a three-core fiber reflection structure is presented. The sensor is composed of a SMF and three-core fiber with a silver reflective film coated on the end face. The sensitivity and stability of the sensor have been investigated in detail and the results are discussed.

## 2 Preparation and principle of sensor

First, the three-core fiber (TCF, Wuhan Senhui Optoelectronic Technology Co., Ltd., China) was cut into the required length, and the two end faces were cut flat. Second, a layer of silver film was coated on the outer surface of TCF by silver mirror reaction. Finally, the other end face of TCF was fused with the SMF with the fusion procedure of the optical fiber fusion splicer. So the required sensing element was obtained. The sensing structure of the liquidlevel sensor is shown in Figure 1(a). The cross-section of the TCF is shown in Figure 1(b). The three cores form a shape of equilateral triangle. The diameters of the cladding and cores of TCF are 125 and 8.6 µm, respectively. The distance between the two cores is about 41.5 µm. The mode of light in SMF will be converted into core mode and cladding mode at the fusion point between the SMF and TCF because of the mode mismatch. The two modes will be reflected by silver film on the end surface of TCF, then propagated through the TCF and eventually coupled into SMF.

The propagation process of optical power from SMF to TCF has been simulated by beam propagation method (BPM). In this model, the lengths of SMF and TCF are 1 and 30 mm, respectively. Figure 2(a) shows the optical power distribution of the cross section near the interface between SMF and TCF. The optical power is first transmitted from SMF to the cladding of TCF to excite the cladding mode. The light distribution of the cross section at the position of 12.5 µm near the fusion point in TCF is shown in Figure 2(b), which illustrates that the light beam gradually enter the three cores at this position to stimulate the fiber-core mode. The light distribution at the end surface of TCF is shown in

Figure 2(c), which indicates stronger optical power in cladding, compared with the three cores. As shown in Figure 2(d), there are more light distribution in the cladding than that of the core.

The interference pattern is formed by the interference between core mode and cladding mode, and its intensity can be expressed as [16],

$$I = I_{core} + \sum I_{clad}^{m} + 2 \sum_{m} \sqrt{I_{core} I_{clad}^{m}} \cos \phi^{m}$$
 (1)

where  $I_{core}$  and  $I_{clad}^{m}$  are the total light intensities of core mode in the three cores and the light intensity of the *m*thcladding mode, respectively.  $\Phi^m$  is the phase difference between the core and the mth-cladding mode, which is proportional to the length of the TCF and the effective refractive index difference between the core and the mthcladding mode, and it can be expressed as [19],

$$\phi^{m} = \frac{4\pi \left(n_{eff}^{core} - n_{eff}^{clad, m}\right)L}{\lambda} = \frac{4\pi \Delta n_{eff}^{m}L}{\lambda}$$
(2)

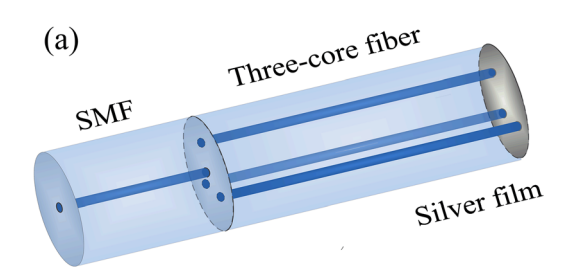
where  $n_{eff}^{core}$  and  $n_{eff}^{clad,m}$  are, respectively, the effective refractive indices of the core mode and the mth-cladding mode.  $\Delta n_{eff}^m$  is the difference of the effective refractive index between the core mode and the mth-cladding mode. L is the length of the TCF, and  $\lambda$  is the monitoring dip wavelength. According to the interference theory, the attenuation peak of the interference can be expressed as [20],

$$\lambda_m = \frac{4\Delta n_{eff}^m L}{2n+1} (n = 0, \pm 1, \pm 2, ...)$$
 (3)

During the liquid-level detection, one part sensing length of sensor will be exposed in the air and the other sensing length will be immersed in liquid. The effective refractive index of the cladding will change with the increase of the liquid level, which lead to the change of the interference wavelength. The shift of the interference wavelength can be expressed as [21],

$$\lambda_{m}^{'} = \frac{4\pi\Delta n_{eff}^{m} (L - L_{h})}{(2n+1)\pi} + \frac{4\pi\Delta n_{eff}^{m} L_{h}}{(2n+1)\pi}$$
(4)

where  $L_h$  and  $\Delta n_{effn}^m$  are the length of the three-core fiber immersed in the liquid and the difference of the effective



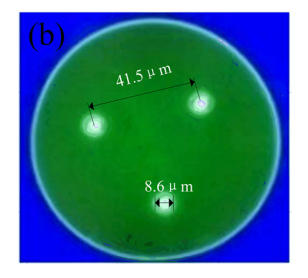


Figure 1: (a) Sensing structure and (b) the end face of TCF.

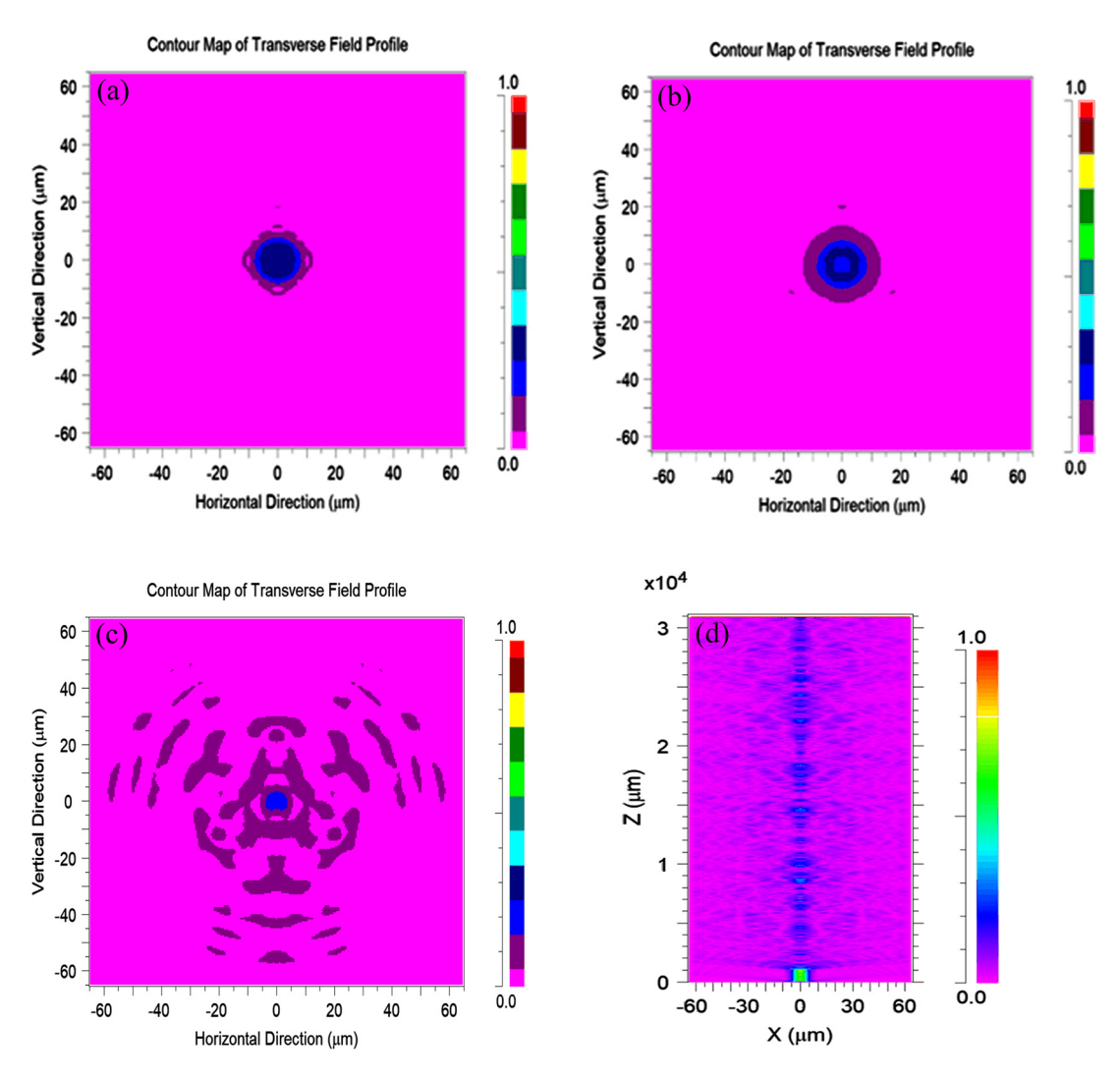


Figure 2: (a) Z-direction cross-sectional light distribution near the interface of SMF and TCF, (b) Z-direction cross-sectional light distribution at 0.125 mm of TCF, (c) Z-direction cross-sectional light distribution at the end of the sensor and (d) XZ cross-sectional light distribution.

refractive index between the core mode and the mthcladding mode, respectively.

#### 3 Results and discussion

The schematic diagram of the liquid-level measuring system is shown in Figure 3. The silver mirror reaction was adopted to coat silver film on the end face of TCF. The other end face of TCF was spliced with SMF by the optical-fiber fusion splicer (S178C, Furukawa Electric, Japan). The sensing part was fixed in parallel on the ruler, and placed vertically in the beaker with designed liquid. In order to facilitate the observation of the liquid-level change, the end of the optical fiber is parallel to the zero scale of the ruler, which is regarded as the zero scale of the liquid level.

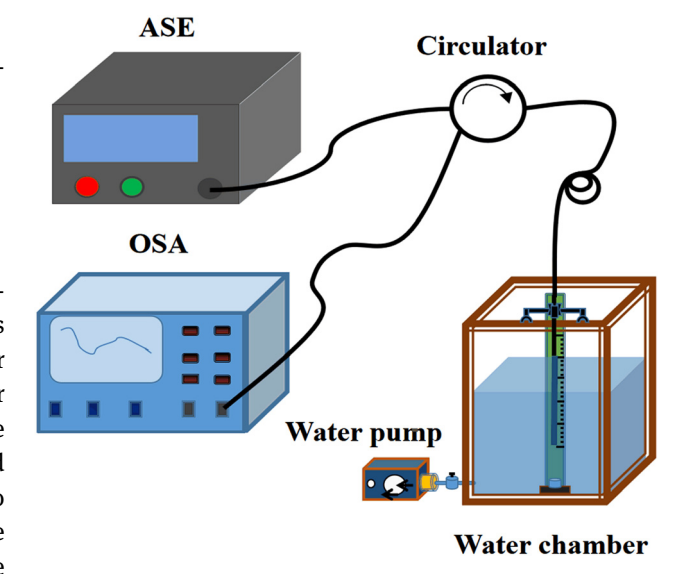
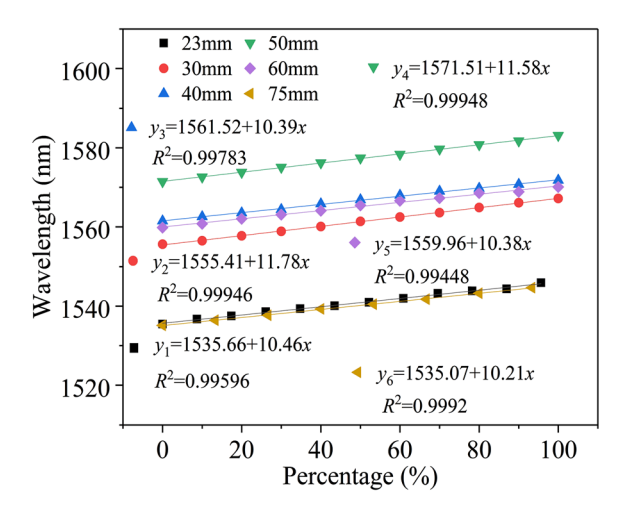


Figure 3: Schematic diagram of the liquid-level measuring system.



**Figure 4:** The relationship between the percentage change of the liquid-level depth measured by different TCF lengths vs. the length of the sensing region and the wavelength shift.

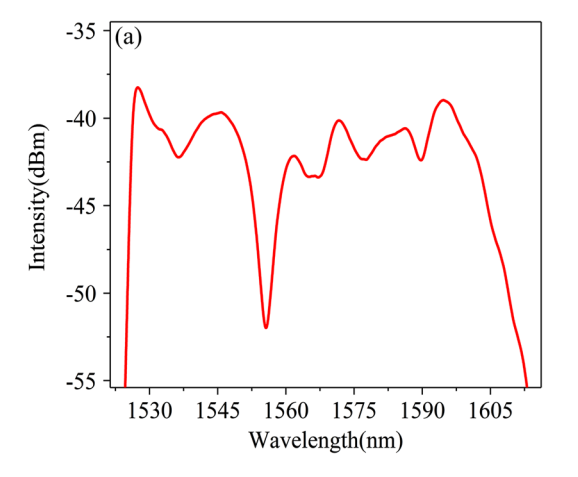
The light beam (wavelength range from 1520 to 1620 nm) first passes through the circulator and transmitted from the SMF to TCF, and reflected by the silver film, then the final reflected light coupled into the SMF at the spliced region and finally output by the circulator to the optical spectrum analyzer (OSA).

The effect of the sensing length of TCF on the sensitivity of sensor was investigated. The water level has been tested by the sensor with the sensing length of 23, 30, 40, 50, 60 and 75 mm at room temperature. The sensitivity of sensor varies with the sensing length. In order to compare the difference in sensitivity of the liquid-level sensor with different sensing lengths intuitively, the change in the liquid-level depth detected by the sensor is converted into a percentage of liquid-level change to sensing length. As

shown in Figure 4, the change in dip wavelength shift shows a similar trend and maintains good linearity at different sensing lengths with the wavelength shift between 10 and 12 nm according to the fitted data. It can be seen that the length of TCF will affect the sensitivity of the liquid-level sensor, which decrease with the increasing of the sensing length of TCF. Therefore, the appropriate sensing length will be adopted according to the testing environment.

As shown in Figure 5(a), the initial spectrum of the sensor with sensing length of 30 mm for TCF in the air is chosen. It can be observed that a wide free spectral region and an obvious monitoring dip appeared under this case. Figure 5(b) shown the wavelength shift of light beam with different water depths at the condition of 30 mm sensing length and 3 mm interval of the water depth. The obvious redshift of the dip wavelength was obtained with the increasing of the water depth. The high sensitivity of 392.83 pm/mm and excellent linearity of 0.99946 are obtained, which are much higher than the sensitivity of –43.7 and 77 pm/mm proposed by Yun et al. and Diaz et al. [12, 13]. Therefore, the sensing length of TCF will be set at 30 mm in the following investigation.

The influence of the sensitivity of presented sensor with refractive index of liquid was also tested. Four different NaCl solutions with concentrations of 0, 5, 10 and 15% were used for liquid-level testing, which corresponding to the refractive index of 1.3333, 1.3424, 1.3510 and 1.3609. As shown in Figure 6(a), the sensitivity of the sensor is increased with the increasing of liquid refractive index though our experiment data, and the different wavelength drift was obtained under different refractive indices too. As shown in Figure 6(b), the response of the liquid-level sensitivity of the sensor to the refractive index



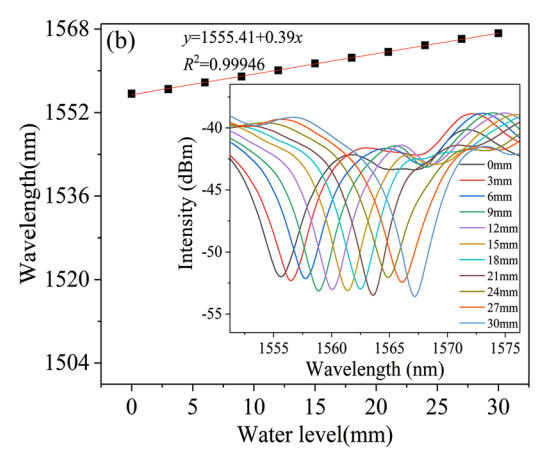


Figure 5: (a) The spectrum of the sensor in the air when the TCF is 30 mm, and (b) the dip wavelength varies with the liquid level.

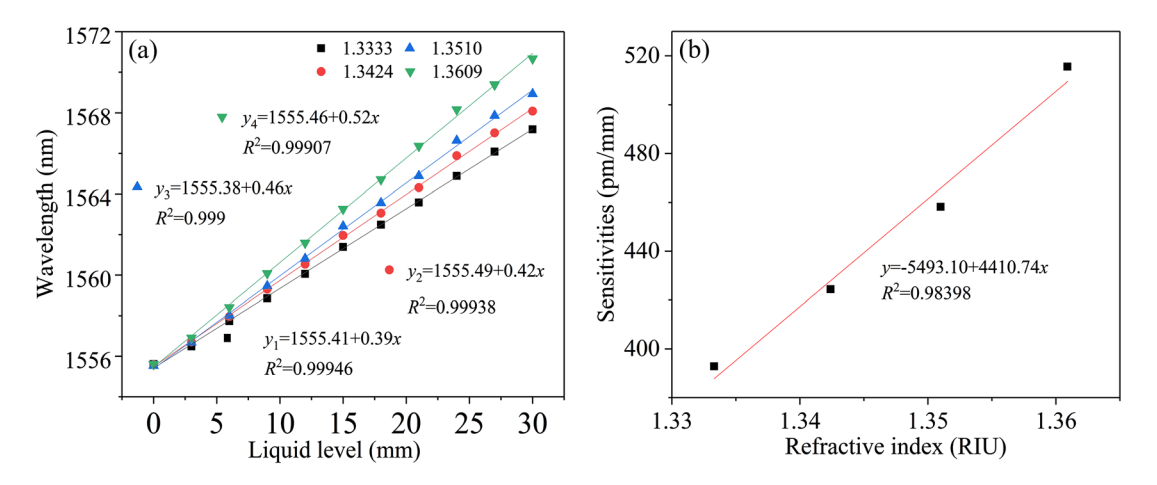


Figure 6: (a) The sensitivity of the sensor in NaCl solutions with refractive indices of 1.3333, 1.3424, 1.351 and 1.3609, respectively, and (b) the sensitivity of the refractive index.

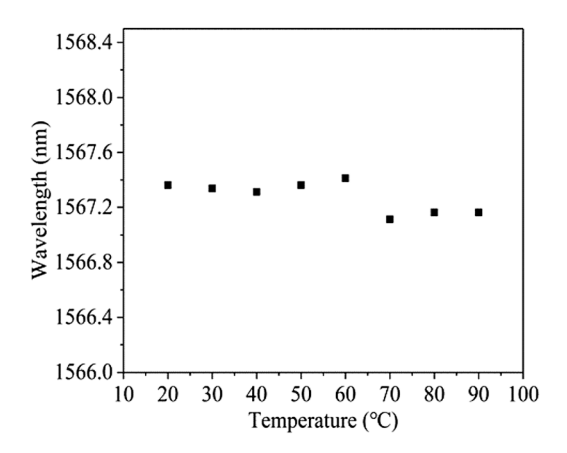


Figure 7: Temperature sensitivity of the sensor.

is 4410.74 pm/mm/RIU, and the linearity is 0.98398. It shows that the refractive index of the liquid can be tested according to the sensitivity of the sensor at same liquid level, which expands the application range of the sensor.

In order to explore the effect of temperature on the performance of the sensor, the temperature stability of the sensor was studied. An appropriate amount of deionized water was added to the beaker and turned off the heating device until the water was heated to boiling. Putting the sensor vertically and submerging it, recording the spectral data every 10 °C from 90 to 20 °C. The measured results are shown in Figure 7. The monitoring wavelength appears no drift with temperature, which show maximum shift of 0.3001 nm. It indicates that the sensor can be used at different temperatures without other additional influence.

As shown in Table 1, compared with other fiber-optic Michelson liquid-level sensors with different structures, our sensor has higher sensitivity (392.83 pm/ppm). In

**Table 1:** Performance comparisons of different fiber-optic Michelson liquid-level sensors.

Structure	Liquid/water- level sensitivity (pm/mm)	Measuring range (mm)	References
In-fiber quasi- Michelson interferometer	-68.3	30	[16]
Michelson interferometer with the core-	77	40	[17]
A probe based on MI viadual-mode elliptical multilayer-core fiber	-33.48	45	[18]
Three-core fiber reflec- tion structure	392.83	30	this work

addition, the simple sensing structure reduces the influence of temperature.

### 4 Conclusions

In summary, a simple optical fiber liquid-level sensor based on Michelson interference structure was proposed. The sensor has excellent sensitivity and linearity. The change of refractive index around the TCF due to different liquid level will affect the cladding mode of TCF, which in turn lead to redshift of the dip wavelength. The sensing range and sensitivity of the sensor can be controlled by the sensing length of TCF. The response of the liquid-level sensitivity of the sensor to the refractive index of NaCl

solution is 4410.74 pm/mm/RIU, which show the sensitivity of sensor increase with the increasing of liquid refractive index. The temperature sensitivity of the sensor is very tiny and can be ignored, which make it can be applied to liquid-level measurement at complex environments.

**Author contribution:** All the authors have accepted responsibility for the entire content of this submitted manuscript and approved submission.

Research funding: The research was supported by the National Natural Science Foundation of China (51574054), Chongging Municipal Education Commission (KJZD-M201901102), Chongging Science and Technology Bureau (cstc2018jcyjAX0294, CSTCCXLJRC- 201905), the Venture & Innovation Support Program for Chongging Overseas Returnees (cx2019092), Science and Technology Bureau of Banan District (2018TJ12, 2019TJ08).

Conflict of interest statement: The authors declare no conflicts of interest.

#### References

- [1] S. Liu, X. Yang, W. Feng, H. Chen, Y. Tao, and Y. Jiang, "Michelson interferometric hydrogen sulfide gas sensor based on NH2-rGO sensitive film," Z. Naturforch. A, vol. 75, pp. 241-248, 2020.
- [2] F. Reverter, X. Li, G. C, and M. Meijer, "Liquid-level measurement system based on a remote grounded capacitive sensor," Sens. Actuators A: Phys, vol. 138, pp. 1-8, 2007.
- [3] B. Kumar, G. Rajita, and N. Mandal, "A review on capacitive-type sensor for measurement of height of liquid level," Meas. Control, vol. 47, pp. 219-224, 2014.
- [4] K. Chetpattananondha, T. Tapoanoi, P. Phukpattaranont, and N. Jindapetcha, "A self-calibration water level measurement using an interdigital capacitive sensor," Sens. Actuators A: Phys, vol. 209, pp. 175-182, 2014.
- [5] H. Canbolat, "A novel level measurement technique using three capacitive sensors for liquids," IEEE trans. Instrument. Meas, vol. 58, pp. 3762-3768, 2009.
- [6] E. Terzic, R. Nagarajah, and M. Alamgir, "A neural network approach to fluid quantity measurement in dynamic environments," Mechatronics, vol. 21, pp. 145-155, 2011.
- [7] J. Peng, W. Feng, X. Yang, G. Huang, and S. Liu, "Dual Fabry-Pérot interferometric carbon monoxide sensor based on the PANI/

- Co<sub>3</sub>O<sub>4</sub> sensitive membrane-coated fibre tip," Z. Naturforsch. A, vol. 74, pp. 101-107, 2019.
- [8] Z. Peng, W. Feng, X. Yang, L. Fang, D. Wei, and X. Liu, "Graphenebased waist-enlarged optical fiber sensor for measurement of sucrose concentration," Z. Naturforsch. A, vol. 74, pp. 751-756, 2019.
- [9] J. E. A. Lopez, J. J. S. Mondragon, P. L. K. Wa, and D. A. M. Arrioja, "Fiber-optic sensor for liquid level measurement," Opt. Lett., vol. 36, pp. 3425-3427, 2011.
- [10] J. Yu, X. Yang, and W. Feng, "Hydrogen sulfide gas sensor based on copper/graphene oxide composite film-coated tapered single-mode fiber interferometer," Z. Naturforch. A, vol. 74, pp. 931-936, 2019.
- [11] K. R. Sohn, and J. H. Shim, "Liquid-level monitoring sensor systems using fiber Bragg grating embedded in cantilever," Sens. Actuators A: Phys, vol. 152, pp. 248-251, 2009.
- [12] B. F. Yun, N. Chen, and Y. P. Cui, "Highly sensitive liquid-level sensor based on etched fiber Bragg grating," IEEE Photon. Technol. Lett., vol. 19, pp. 1747-1749, 2007.
- [13] C. A. R. Diaz, A. G. L. Junior, P. S. B. Andre, et al., "Liquid level measurement based on FBG-embedded diaphragms with temperature compensation," IEEE Sensor. J., vol. 18, pp. 193-200, 2017.
- [14] G. Onorato, G. Persichetti, I. A. Grimaldi, G. Testa, and R. Bernini, "Optical fiber fuel level sensor for aeronautical applications," Sens. Actuators A: Phys, vol. 260, pp. 1-9, 2017.
- [15] P. L. Swart, "Long-period grating Michelson refractometric sensor," Meas. Sci. Technol., vol. 15, p. 1576, 2004.
- [16] Q. Z. Rong, X. G. Qiao, Y. Y. Du, et al., "In-fiber quasi-Michelson interferometer for liquid level measurement with a corecladding-modes fiber end-face mirror," Optic Laser. Eng., vol. 57, pp. 53-57, 2014.
- [17] P. F. Li, H. T. Yan, and H. J. Zhang, "Highly sensitive liquid level sensor based on an optical fiber Michelson interferometer with core-offset structure," Optik, vol. 171, pp. 781-785, 2018.
- [18] X. Liang, G. B. Ren, Z. B. Liu, H. Wei, and S. S. Jian, "In-fiber liquid-level probe based on Michelson interferometer via dualmode elliptical multilayer-core fiber," J. Mod. Optic., vol. 63, no. 13, pp. 1254-1259, 2016.
- [19] Z. Y. Li, Y. P. Wang, C. R. Liao, et al., "Temperature-insensitive refractive index sensor based on in-fiber Michelson interferometer," Sensor. Actuator. B Chem., vol. 199, pp. 31-35,
- [20] C. Li, T. G. Ning, C. Zhang, et al., "All-fiber multipath Mach-Zehnder interferometer based on a four-core fiber for sensing applications," Sens. Actuators A: Phys, vol. 248, pp. 148-154, 2016.
- [21] L. C. Li, L. Xia, Z. H. Xie, and D. M. Liu, "All-fiber Mach-Zehnder interferometers for sensing applications," Optic Express, vol. 20, pp. 11109-11120, 2012.